Finite Difference Time Domain Simulation of the Outer Ear

Sebastian Schmidt, Herbert Hudde
Institut für Kommunikationsakustik (IKA), Ruhr-Universität Bochum, D-44780 Bochum, Germany
Email: sebastian.schmidt@rub.de, herbert.hudde@rub.de

Introduction

At the IKA in Bochum, a comprehensive finite element (FE) model of the peripheral hearing organ is developed. It is designed to simulate the complex behaviour and interaction of bone, tissue and fluid parts in the human head (BOHEAR). A finite differences (FD) simulation was programmed to efficiently solve the wave equation in the surrounding of the head. The model was studied to analyse its advantages in contrast to the FE discretisation method. When a system is known to have a short impulse response, time domain simulations are expected to be more efficient than a frequency domain approach. These systems include reflection-free terminated acoustic ducts and free field wave propagation geometries, in particular sound fields concerning the ear canal and the outer ear. Provided that the transient response has decayed under a predefined limit, all relevant information about the acoustic system of interest is gathered. A Fourier transform of the calculated time functions yields frequency domain results.

Implementation of the FD model

Algorithm and model design

The implementation of the FD simulation follows a suggestion of Botteldooren [1]. The wave equations of the pressure p and the velocity v in time t and space x

$$\frac{\partial p}{\partial x} = -\varrho \frac{\partial v}{\partial t} \quad \text{and} \quad \frac{\partial v}{\partial x} = -\frac{1}{c^2 \varrho} \frac{\partial p}{\partial t} \tag{1}$$

are discretised. Equation 1 represents the one-dimensional case with the velocity of sound c and the fluid density ϱ. A difference approximation like

$$\frac{\partial p}{\partial x} \simeq (p_{n+1} - p_n)/\Delta l \tag{2}$$

at sampling points n and $n+1$ is used. With discrete space and time steps (Δl and Δt), one obtains

$$\begin{aligned} v_{n+\frac{1}{2},k+\frac{1}{2}} &= v_{n-\frac{1}{2},k+\frac{1}{2}} - \frac{\Delta t}{\varrho \Delta l}[p_{n,k+1} - p_{n,k}] \\ p_{n+1,k} &= p_{n,k} - \frac{\varrho c^2 \Delta t}{\Delta l}[v_{n+\frac{1}{2},k+\frac{1}{2}} - v_{n+\frac{1}{2},k-\frac{1}{2}}] \end{aligned} \tag{3}$$

as updating equations for the discrete time and space steps n and k, respectively. The differences equation system 3 can be expanded to three dimensions and implemented in C++ directly. The spacially discrete variables of pressure and velocity represent the cells of a rectangular grid as shown in figure 1 for two dimensions. The

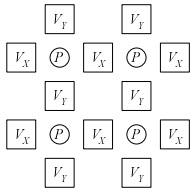

Figure 1: Example of a two-dimensional FD grid with cells representing either local pressures (P) or velocity components (V_X, V_Y).

rational indices $(n+\frac{1}{2}, k+\frac{1}{2})$ correspond to the v-cells which are always centered between the p-cells. Obstacles, walls and the boundary of the simulation space have to be modelled by special velocity cells. On these cells, a boundary admittance can be applied. The values of Δl and Δt determine the tradeoff between accuracy and stability. To guarantee stability, the condition

$$\Delta l \geq \sqrt{N} \cdot c \cdot \Delta t \tag{4}$$

has to be fulfilled [2]. N is the number of dimensions, c means the velocity of sound. Equation 4 states the interrelation between Δl and Δt. To map details of the pinna, space steps in the range of millimeters are necessary. Thereby, the FD system has to work at extremely high sampling rates $f_S = 1/\Delta t$.
The FD model was implemented in C++. For convenience, the geometrical analysis of the objects of interest was carried out with MATLAB.

Grid improvements

When obstacle areas inclined to the cartesian grid are modelled, a significant retardation of collateral waves can be observed. Further investigations show that the staggered boundary configuration in the proximity of the wall causes the error. An improvement of the cartesian FD model was recommended by Botteldooren with the use of voronoi cells. Here, a layer of non-rectangular cells is fit onto the boundaries. The creation of a correct voronoi grid representation, however, remains a serious problem. To solve the problem, local grid refinements in the neighbourhood of the boundaries turn out to be appropriate. In the current FD simulations, two grids with varying space steps Δl were used. At the interface of the different grid configurations, interpolator cells have to be employed. Figure 2 shows some cells of the interface layer. No cell of the fine grid has a direct neighbour in the coarse grid. The interpolator cells provide the missing pressure values by linear interpolation of the surrounding pressure values.

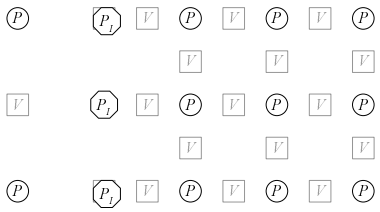

Figure 2: Transition from a coarse (left) to a fine segmentation (right) in an FD grid. The octagonal cells (P_I) represent interpolators that provide pressure values to the adjacent cells of the fine grid. Two interpolators cover velocity cells of the coarse grid.

Absorbing boundaries and sources

The modelling region is bounded by a hemispherical shell. The implementation of the interface layer to free field is programmed using the absorbing layer technique. Therefore, a boundary admittance equal to the free field admittance of plane acoustic waves is provided at each velocity element on the hemispherical boundary region. A faster decay of the impulse response was moreover obtained by fitting the flow source with absorbing elements. For that purpose, the source was implemented by superposition of the source signals with the values contained in the absorbing velocity cells at the source position. With this technique an anechoic membrane moving according to the exitation function is modelled.

Measurements

In addition to the FD model, FE calculations with the commercial software ANSYS were carried out both in time and frequency domain. In order to compare the simulation mechanisms, an artificial pinna was subject of the observation. The pressure distribution on a baffle around the pinna was chosen as evaluation attribute. The studied pinna originates from a Head Acoustics dummy head and was chosen due to the easily reproducable geometry. In addition, acoustic measurements were carried out. An aluminium model of the pinna was mounted onto a board where 12 equally spaced bore holes were drilled on a circle with a radius of 6 cm around the center of the artificial ear canal. Probe microphones were inserted into the bores and a small loudspeaker radiated sound into the ear canal from the back side of the pinna.

Comparison and conclusion

Figure 3 shows measurement and simulation results of the pressure transfer functions between the artificial ear canal and four arbitraryly chosen bores in the baffle. The pressure time functions were transformed using an FFT of 20 Hz resolution. It is difficult to generate similar grid conditions for a fair comparison of the methods. Thus, the *accuracy* of the results with respect to the measurements was adjusted to be alike. Figure 4 shows the transfer function plots of the methods for one of the bores.
The simulation parameters and the calculation times on a reference machine are given in table 1. With its fine grid step, the FD model is bound to extremely high sampling rates due to the stability condition in equation 4. The sampling rate determines the number of calculations which are necessary to simulate the decay time of the impulse response. The FE model features a drastically increased element edge length in comparison with the FD approach. Stability or accuracy are not affected.
The two time domain models show shorter calculation times than the frequency domain model. Summing up, the FD model yields similar calculation times as the FE approaches. The present FD algorithm could be improved by using a better adaptation of the grid resolution to the problem considered. An optimised FD approach is expected to be more efficient than the FE method in time domain. However, it is restricted by the need for stability and fine grids near boundaries.

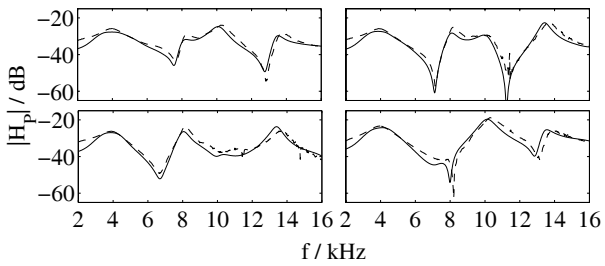

Figure 3: Pressure transfer functions between the artificial ear canal and four arbitraryly chosen bore holes (FD: solid line; measurement: dashed line)).

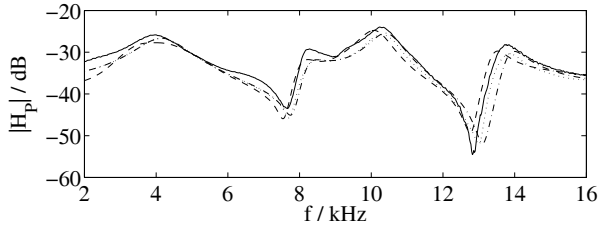

Figure 4: Results of the models (FD: dashed line; FE in time domain: dotted line; FE in frequency domain: dash-dotted line) and the measurement (solid line).

	FD	FE-TD	FE-FD
Elem. edge length	0.3-0.6 mm	2-5 mm	2-5 mm
Time step	0.55 μs	4.9 μs	
Sampling frequency	1.8 MHz	0.2 MHz	
Frequency step			20 Hz
No. of calculations	4500	450	800
Calculation time	5.5 h	4.4 h	8.9 h

Table 1: Simulation parameters (FE-TD and FE-FD refer to FE method in time and frequency domain, respectively.).

References

[1] Botteldooren, D. (1994): Acoustical finite-difference time-domain simulation in a quasi-Cartesian grid, J. Acoust. Soc. Am. 95 (5), 2313-2319

[2] Strikwerda, J. C. (1989): Finite difference schemes and partial differential equations, Wadsworth & Brooks/Cole, Belmont, California